Journal of South American Earth Sciences 107 (2021) 103020

Contents lists available at ScienceDirect

Journal of South American Earth Sciences

journal homepage: www.elsevier.com/locate/jsames

Mercury chemostratigraphy as a proxy of volcanic-driven environmental changes in the Aptian-Albian transition, Araripe Basin, northeastern Brazil

Ana Paula A. Benigno [a,b,*], Antônio Á.F. Saraiva [c], Alcides N. Sial [d], Luiz D. Lacerda [a]

[a] LABOMAR, Institute of Marine Sciences, Federal Univ. of Ceará, Fortaleza, CE, 60165-081, Brazil
[b] IFCE, Federal Institute of Ceará, Campus Umirim, Umirim, CE, 62660-000, Brazil
[c] Department of Physical and Biological Sciences, Regional Univ. of Cariri, Crato, CE, Brazil
[d] NEG–LABISE, Dept. of Geology, Federal Univ. of Pernambuco, Recife, PE, 50740-530, Brazil

ARTICLE INFO

Keywords:
Mercury
Araripe basin
Stable isotopes
Organic carbon
Biological crisis

ABSTRACT

The stratigraphy of mercury (Hg) in sections of the Araripe Basin straddling the Aptian-Albian transition, encompassing the Romualdo, Ipubi, Crato and Barbalha (formerly Rio da Batateira)Formations showed positive excursions of Hg concentrations without correlation with organic carbon (C-org) contents. These incursions occurred during the deposition of the Barbalha Formation, which occurred in the Aptian under warm climate and high bio-productivity; in the Crato Formation, in the Albian, and also during the deposition of the Romualdo Formation. The Hg enrichments suggest external sources of Hg to the basin. The positive Hg excursion in the Ipubi Formation, unlike the others, was shown to be correlated with an increase in the deposition of C-org, suggesting internal processes as major river of Hg accumulation in sediments. The positive Hg excursions independent of C-org accumulation are concomitant to periods of intense volcanic activity in the Kerguelen Large Igneous Provinces (LIP). The excursion observed in the Ipubi Formation, however, seems associated with an event of anoxia, resulting in sediments rich in C-org, scavenging Hg from the water column. The Hg chemostratigraphy helps to understand of the paleoenvironmental changes in the Araripe basin, allowing understanding some of the drivers of such changes as the influence of volcanic activity and events of anoxia, as well as major biological crises.

1. Introduction

The Araripe Basin had its origin and evolution related to tectonic events resulting in the rupture and fragmentation of Gondwana and the opening of the South Atlantic Ocean and its filling during the Mesozoic. It is the largest sedimentary basin in the Brazilian northeast hinterland, hosting one of the world largest fossil diversity from the Jurassic-Cretaceous period (Coimbra et al., 2002a,b; Fara et al., 2005; Fambrini et al., 2011). The basin harbors the Geopark Araripe, the first in the Americas recognized by the Global Geopark Network due to the relevance of its fossil record in excellent preservation state (Mochiutti et al., 2012).

This geological interval was highly complex with episodes of oceanic crust creation, warming punctuated by rapid cooling events, ocean anoxia (OAE), increasing volcanic activity and the formation of large igneous provinces (LIP) (Bralower et al., 1994, 1999; Keller, 2008). During the Aptian-Albian interval (~100–125 Ma) there were significant climatic, tectonic and sea level changes with strong impacts on marine planktonic communities (Sabatino et al., 2018) triggering perturbations of the Carbon cycle leading to ocean anoxic events (OAE). These have been associated with peaks of intense and widespread volcanic activity, the formation of oceanic rises and submarine mountain chains and continental basalts (Bralower et al., 1999; Sabatino et al., 2018). However, uncertainties in age definition during this interval hampers direct cause-effect links of these events, but massive release of $CO_2$by volcanism, resulting in a generalized warming during the middle Cretaceous and the enrichment of mantle-derived materials such as trace metals, in particular volatile ones as mercury (Hg) (Bralower et al., 1999).

Coincidence of radiometrical dating of LIPs and mass extinctions and OAE episodes strongly suggests a causal relationship, due to the enormous amount of magma released during these catastrophic impacts of the climate and ocean conditions (Courtillot and Renne, 2003; Bond and Wignall, 2014; Percival et al., 2015; Sabatino et al., 2018), but the

* Corresponding author. LABOMAR, Institute of Marine Sciences, Federal Univ. of Ceará, Fortaleza, CE, 60165-081, Brazil.
E-mail address: lldrude@pq.cnpq.br (L.D. Lacerda).

https://doi.org/10.1016/j.jsames.2020.103020
Received 11 June 2020; Received in revised form 4 November 2020; Accepted 5 November 2020
Available online 13 November 2020
0895-9811/

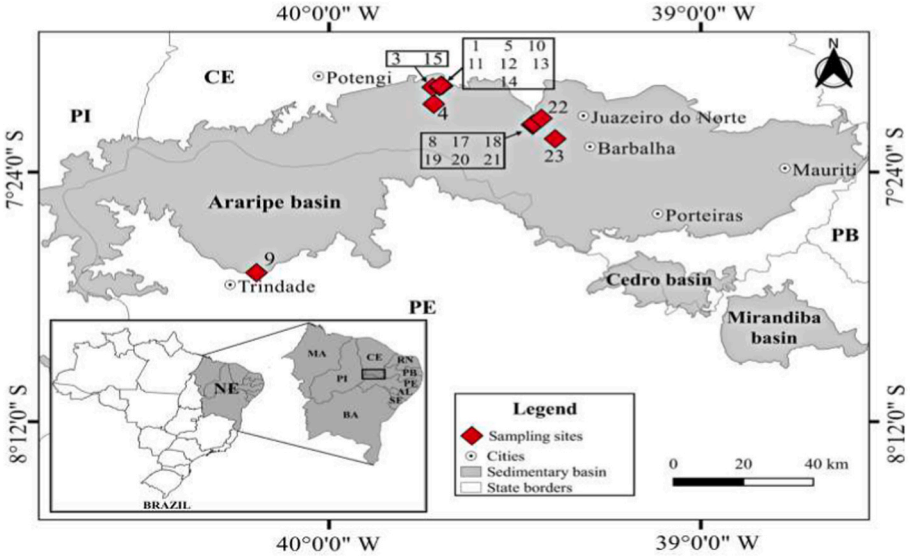

Fig. 1. Geological map of the Araripe Basin in Northeastern Brazil showing major cities, states limits and sampling stations in the different Formations.

mechanisms involved are still debatable. Among the many proxies of LIPs activities, Hg stratigraphy, in conjunction with C and O stable isotopes, has proved a reliable tracer of LIPs allowing the correlation between volcanism and biological crises and catastrophic environmental changes (Sanei et al., 2012; Sial et al., 2013, 2016, 2018; 2016; Percival et al., 2017; Grasby et al. 2013, 2016).

Despite the numerous studies on the geology and fossil record of the Araripe Basin, a very scarce literature exists on geochemistry and none, to our knowledge, on Hg stratigraphy. This present study deals with these later aspects of the Araripe Basin and uses, for the first time, stable isotopes, C-org and Hg stratigraphy to understand local and distal drivers of environmental changes, in particular of volcanisms, with emphasis on the Aptian-Albian interval (Fig. 1) and its eventual association with local biological crises.

2. Geological setting

The Araripe Basin is located between the states of Ceará, Pernambuco and Piauí in northeastern Brazil (Fig. 1), comprising an area of approximately 9000 km^2, being considered the most extensive sedimentary basin in northeastern Brazil (Assine, 1992; Valença et al., 2003; Neumann et al., 2008; Costa et al., 2014; Saraiva et al., 2016; Fabin et al., 2018). The geological history of this intracratonic basin began about 150 Ma ago and is associated with the separation of Gondwana and the opening of the South Atlantic (Ceará State Government, 2012). The Araripe Basin stands out for its extension in area and stratigraphic amplitude, comprising four tectonostratigraphic phases called synecise, pre-rift, rift and post-rift South Atlantic (Assine, 1994; 2007; Martil et al., 2007; Fambrini et al., 2011; Paula-Freitas and Borghi, 2011; Camacho and Oliveira e Sousa, 2017).

The section addressed in the present study offers a stratigraphic record for the Upper Aptian and Lower Albian range, with sediment samples from the Barbalha (Formerly Rio da Batateira Formation) (113 Ma), Crato (112 Ma), Ipubi (108 Ma) and Romualdo (100 Ma) Formations. It is noteworthy that the dates mentioned above correspond to relative dates available by the Ceará State Government (2012), and although they represent a limitation regarding the more precise positioning of the formations of the Araripe Basin in the geological scale of time, they are considered due to the absence of absolute dating for all formations. However, Coimbra et al. (2002a,b) suggested, based on the microfossil occurrence in the Barbalha and Santana formations as well as palynomorphs of the Arajara Formation, that the Alagoas local stage is upper Albian for the first two formations and Aptian/Albian for the Ipubi and Romualdo members of the Santana Formation, correlating well with the nearby basin of the northeastern Brazil. Among the forms found in the deposits of the Jatobá basin, the species of the genus *Pattersoncypris* and *Damonella grandiensis* n. sp. are key fossils of the Aptian and the lower Albian (Alagoas local stage) which provide the first record of this interval in the Jatobá basin (Tomé et al., 2014). Most of the fossil recorded to now, therefore, supports the dating use in this present study. The stratigraphy of the Araripe Basin used in this study followed Fambrini et al. (2019). A brief description of the studied formation is presented.

2.1. Barbalha Formation

The Barbalha Formation is the first Aptian-Albian section corresponding to a transgressive phase of the rifting sequence presenting a vertical stratigraphic profile including two fluvial-lacustrine cycles, the first typically fluvial while the second typically lacustrine. It is a fining-upward sequence, with medium to coarse, even conglomeratic arenites at the base, which pass into silty shales with medium-grained sandstone interbeds up section. The cycle ends in black pyro-bituminous shales, enriched in carbonate layers of algal origin and containing coprolites, ostracods, fish remains and pollen and plant fragments (Valença et al., 2003).

This interval, also called the Araripe plumbiferous sequence, presents sulfides within mineralized limestones, evidencing the end of an event of reduction of transport capacity of rivers allowing fine-grained sediment deposition. This characterizes a confined environment, under reducing conditions, caused by low oxygenation of the waters, facilitating the precipitation of sulfides rich in lead, copper and zinc that easily settled in the limestones present in this section. In the pyrobituminous shales of the Barbalha Formation, facies of thin dense sandstones occur again, with the same characteristics as the sandstones of the base (Chagas et al., 2007; Rios-Netto et al., 2012). The Barbalha Formation is an important regional stratigraphic marker horizon of the Araripe Basin, as it represents the record of the onset of the first lake system in the basin characterized by anoxic conditions, which led to the preservation of significant amount of organic matter (Assine, 2007; Assine et al., 2014). Palynomorphs (pollen) preserved in these sediments suggest a dry, warm semiarid climate (Chagas et al., 2007).

2.2. Crato Formation

The Crato Formation has a thickness of 50 m and overlies the

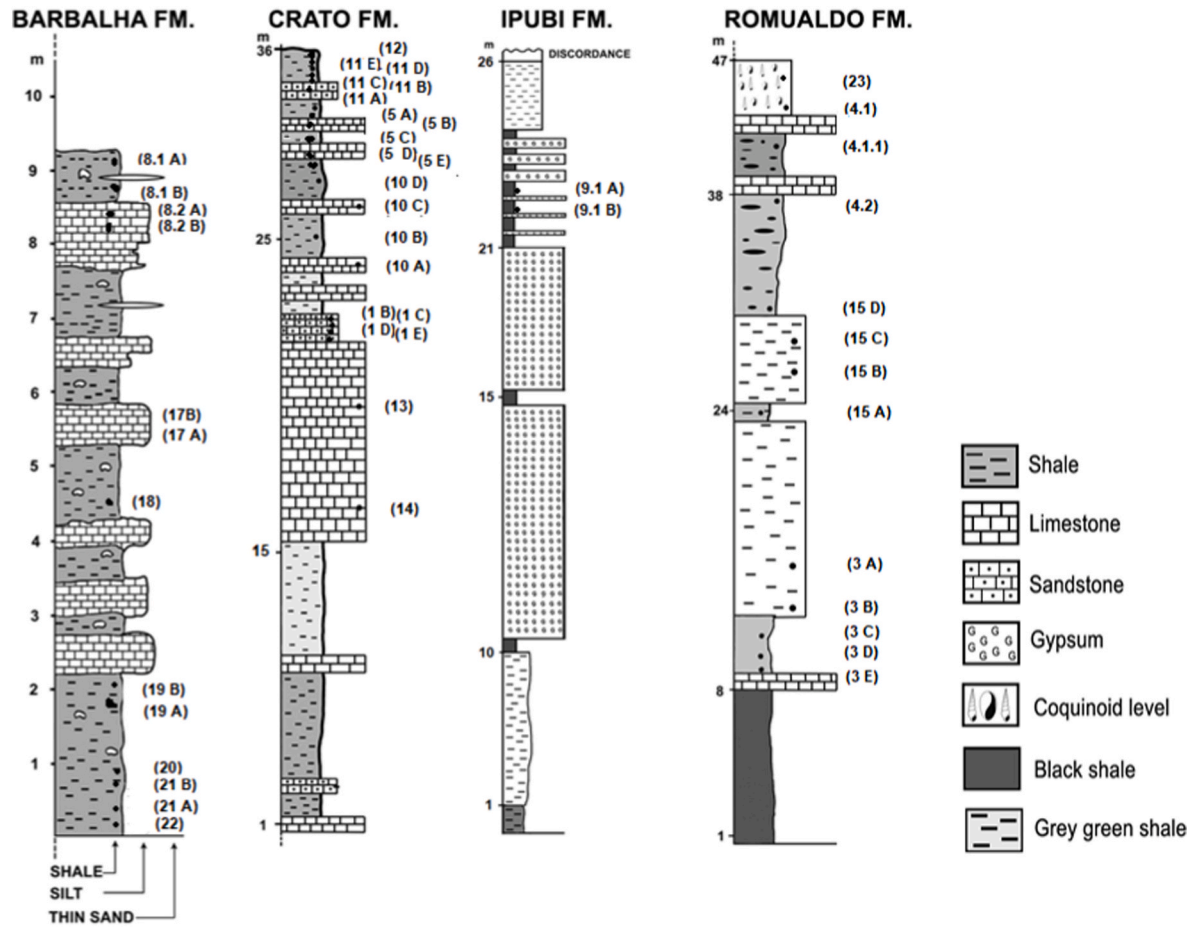

Fig. 2. Simplified stratigraphic profile of the Araripe Basin detailing the sampled sections, stratigraphic height and location of samples (in parentheses), based on and adapted from Coimbra et al. (2002a,b) Carmo et al. (2004), Fara et al. (2005) and Saraiva et al. (2015).

Barbalha Formation that gradually changes into parallel, fine, horizontal laminated marls. This Formation, is well known because of its exceptionally well preserved fossil record, the most diversified fossil assemblage from the non-marine Cretaceous, including a large diversity of birds, insects, plants and even pterodactyls (Kellner 2002; Santana et al., 2013; Martill et al., 2007; Saraiva et al., 2015). Sediment deposition occurred during the Lower Cretaceous(~113–115 Ma), displaying a sequence of lacustrine limestone interbedded by siliciclastic facies, deposited in a saline lacustrine environment (Assine, 2007) or even a hypersaline lagoon with restricted connections to the sea (Varejão et al., 2016). This scenario allows the occurrence of marine organisms in the shallow parts of the lake (Barbosa et al., 2004). Some authors, however, suggest a non-marine deposition in a saline lacustrine environment with episodic freshwater input and shallow water bodies with low energy and depositional environments characterized by high sedimentation rates (Sayão and Kelnner, 2006).

2.3. Formação Ipubi

Above the laminated limestones of the Crato Formation is the Ipubi Formation (Valença et al., 2003), which comprises siliciclastic and evaporite rocks of origin related to a brine concentration cycle followed by dilution of sea salt (Castro et al., 2006), being deposited possibly under conditions of arid to semi-arid climate. The Ipubi Formation is characterized by a shallow post-rift marine-lacustrine environment (Castro et al., 2006; Fabin et al., 2018) deposited in the supratidal region of an Aptian-Albian lagoon system. Thus, these sediments are considered as deposits of restricted, evaporitic lagoon basins, where periodic flooding by marine waters occurred and was subjected to intense evaporation, which provided the concentration of salts.

The Ipubi Formation is composed essentially of discontinuous bodies of gypsum and anhydrite with a thickness of approximately 30 m, interbedded with black pyrobituminous shales, with high organic matter content containing pyrite crystals (Assine et al., 2014). These contain non-marine shells, ostracodes, charred plant fragments and pyritized fish and chelonians fossils (Barros et al., 2016). A shallow coastal environment has been proposed a few square kilometers in area, but with no connection to the sea, similar to the modern salt pans existing in South Australia, for example (Assine, 1992; Assine et al., 2014). The recognition of the Ipubi Formation is difficult in view of the discontinuity of the layers and the difficulty in setting limits of the precipitates.

2.4. Romualdo Formation

In the Albian, there was a transgressive pulse that caused the interruption of the evaporites of the Ipubi Formation, diluting the hypersaline brines and causing the sedimentation of shales, carbonates and marls of the Romualdo Formation. The Romualdo Formation is approximately 120 m thick, and overlies sandstones and dark shales that cover the gypsum deposits of the Ipubi Formation. It is, in turn, overlain by reddish siltstones of the Arajara Formation. The lower part of the Romualdo Formation consists predominantly of interstratified sandstones and pyrobituminous shales. To the top, the stacking is transgressive and the coastal sandstones give way to a section of shales, rich in ostracodes, pollen grains, spores, dinoflagellates, foraminifera and mollusks typical of coastal environments, such as estuaries and lagoons, with periodic marine transgressions, indicating the unquestionable influence of the sea. The shales acquire, progressively towards the top,

Table 1
Mercury (Hg), $\delta^{13}C$, $\delta^{18}O$, TOC, Hg/TOC and Mn/Sr ratios from the Araripe Basin, NE Brazil.

Formation	Samples	Ma	Hg (ng g^{-1})	$\delta^{13}C$ (VPDB ‰)	$\delta^{18}O$ (VPDB ‰)	TOC (%)	Hg/TOC	Mn/Sr
Romualdo Formation	23	**100**	2.52 ± 0.36	−1.61	−10.11	0.56 ± 0.10	4.48	10.1
	4.1		5.60 ± 0.61			1.42 ± 0.01	3.95	
	4.1.1		5.13 ± 0.30			1.41 ± 0.11	3.64	
	4.2		12.57 ± 1.20	−11.53	−6.23	1.21 ± 0.25	10.40	2.6
	15 D		1.54 ± 0.24			0.84 ± 0.09	1.85	
	15C		1.96 ± 0.44			0.62 ± 0.06	3.13	
	15B		3.08 ± 0.20			0.73 ± 0.01	4.22	
	15A		6.94 ± 0.35			1.00 ± 0.14	6.96	
	3A		1.11 ± 0.22	−9.14	−5.26	0.50 ± 0.05	2.22	4.4
	3B		26.33 ± 0.76			0.67 ± 0.01	39.30	
	3C		8.76 ± 0.20	−10.89	−6.40	0.84 ± 0.05	10.43	5.1
	3D		2.80 ± 0.22	−10.79	−6.04	0.68 ± 0.01	4.12	5.2
	3E		2.31 ± 0.29			0.49 ± 0.17	4.71	
Ipubi Formation	9.1 (A)	**108**	20.37 ± 0.44	−8.15	−4.77	13.85 ± 0.62	1.47	4.7
	9.1 (B)		8.91 ± 0.23	−4.81	−3.40	3.05 ± 0.10	2.92	< ld
Crato Formation	12	**112**	19.83 ± 1.09			0.63 ± 0.04	31.38	
	11E		12.49 ± 1.44	−5.69	−5.32	0.45 ± 0.04	27.47	10.0
	11D		9.00 ± 0.77	−7.65	−5.17	0.42 ± 0.11	21.35	3.3
	11C		34.17 ± 2.35	−3.47	−6.31	0.32 ± 0.13	106.03	10.0
	11B		7.50 ± 0.25	−5.47	−5.36	0.26 ± 0.00	28.73	< ld
	11A		7.21 ± 0.40	−1.15	−6.25	0.59 ± 0.02	12.20	2.7
	5A		2.45 ± 0.37	−6.81	−6.01	0.80 ± 0.01	3.05	6.6
	5B		1.56 ± 0.19	−8.18	−4.09	0.78 ± 0.08	2.01	< ld
	5C		1.37 ± 0.06			0.95 ± 0.01	1.44	
	5D		4.36 ± 0.17	−7.83	−4.29	1.01 ± 0.05	4.32	< ld
	5E		2.19 ± 0.09	−4.35	−6.79	0.90 ± 0.01	2.44	< ld
	10D		23.12 ± 2.77	−7.16	−3.84	0.25 ± 0.01	90.77	10.8
	10C		3.63 ± 0.40	−0.22	−7.77	0.77 ± 0.13	4.72	1.8
	10B		2.62 ± 0.65			0.39 ± 0.03	6.73	
	10A		6.05 ± 2.14	−6.00	−1.17	0.16 ± 0.00	37.38	3.1
	1B		33.75 ± 4.78	−8.90	−5.38	1.44 ± 0.01	23.44	< ld
	1C		20.69 ± 0.38	−5.68	−5.61	1.67 ± 0.01	12.38	< ld
	1D		39.75 ± 0.98			1.84 ± 0.68	21.59	
	1E		44.04 ± 4.16	−0.33	−7.07	0.54 ± 0.09	81.98	0.7
	13		20.57 ± 0.86	+0.61	−4.52	1.16 ± 0.10	17.81	1.6
	14		7.60 ± 1.28	−2.23	−4.87	0.35 ± 0.11	21.72	0.9
Barbalha Formation	8.1 A	**113**	12.38 ± 2.02			1.90 ± 0.01	6.53	
	8.1 B		3.95 ± 0.12			1.59 ± 0.01	2.49	
	8.2 A		10.41 ± 1.22			2.40 ± 0.01	4.33	
	8.2 B		11.00 ± 0.28			2.05 ± 0.01	5.37	
	17B		16.62 ± 2.57			1.73 ± 0.10	9.61	
	17A		43.60 ± 2.28	+0.72	−8.65	3.28 ± 0.01	13.30	4.7
	18		13.27 ± 0.36			1.42 ± 0.05	9.34	
	19B		5.05 ± 0.26			0.96 ± 0.14	5.24	
	19A		30.63 ± 5.90			1.52 ± 0.06	20.19	
	20		3.47 ± 0.19			0.43 ± 0.08	8.10	
	21B		3.90 ± 0.66			0.32 ± 0.04	12.18	
	21A		2.69 ± 0.15			0.42 ± 0.04	6.42	
	22		3.59 ± 0.21			0.30 ± 0.04	11.87	

darker colors, due to higher contents of organic matter, characterized by the presence of a level with fossiliferous concretions, usually with three-dimensionally preserved macrofossils, which reaches the eastern edge of the Araripe Plateau (Assine, 2007; Saraiva et al., 2007).

This formation presents one of the most important paleontological records of the Early Cretaceous, and the degree of exceptional preservation of fossils has made this paleontological material known at national and international level. The stratigraphic record of the Romualdo Formation is a key element to clarify the paleogeographic and paleoenvironmental scenarios, in response to the fragmentation of the Gondwana and the opening of the South Atlantic Ocean, since this unit revealed a record of an important marine entry in a wide area of northeastern Brazil from neo-Aptian to neo-Albian. The transgression caused profound environmental changes with relevant impacts on local and regional biotas (Kellner, 2002; Fara et al., 2005).

3. Materials and methods

The study analyzed 49 samples collected between 2016 and 2018 in the Araripe Basin; 13 in the Barbalha Formation, 21 in the Crato Formation, 2 in the Ipubi Formation and 13 in the Romualdo Formation. Samples were obtained by careful transversal digging of the respective outcrops, avoiding the superficial weathered surface and are distributed along the Aptian-Albian stratigraphic profile as shown in Fig. 2. Samples were ground to dust after the removal of possible weathering surfaces, homogenized and dried in an oven at 60 °C for 12 h. Dried samples were preserved in hermetically sealed vials in a dry environment, air-conditioned at 20 °C, until analyzes.

Mercury (Hg) concentrations were quantified in duplicate subsamples (0.5 g) after digestion in erlenmeyers of 125 mL, containing 20 mL of *aqua regia* (50% v/v), in a water bath at 70° to 80 °C for 2 h. The erlenmeyers were closed using thermokinetic reactors (cold fingers). The resulting extract was quantitatively transferred to volumetric balloons (50 mL) completed with deionized water (Aguiar et al., 2007). All glassware were previously washed with deionized water in a 10% v/v (10% v/v) solution bath for 24 h and then in an HCl bath (Sigma-Aldrich) 10% v/v for 24 h. Cold Vapor Atomic Absorption Spectrometry (CVAAS) quantified the Hg concentrations in the extracts, with simultaneous analyses of reference material (Estuarine Sediment NIST 1646A) to evaluate the accuracy and recovery of the method. Recovery

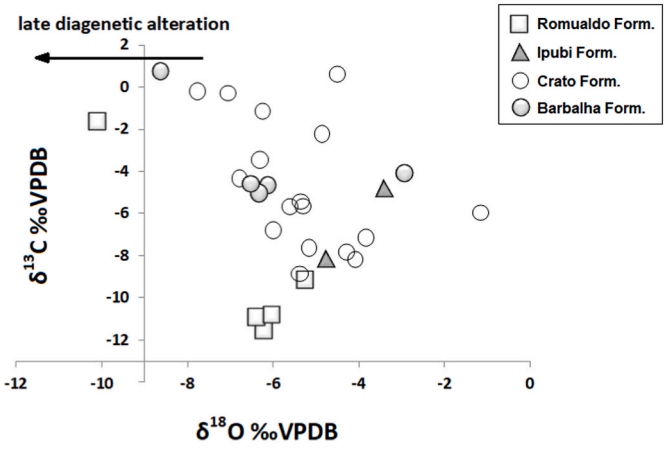

Fig. 3. Graphic plot between $\delta^{13}C$ and $\delta^{18}O$ firstly proposed by Keith and Weber (1964) and modified according to (Schobben et al., 2026). Sample depth according to Fig. 2, but distance between samples in different formations is arbitrary to highlight differences within a single formation.

averaged 78.4 ± 6.6%; the detection limit of the procedure was 0.02 ng g^{-1} Hg and the quantification limit of 0.06 ng g^{-1}.

The concentrations of Mn and Sr were quantified in subsamples of approximately 0.5 g mixed in teflon tubes with 20 mL Aqua Regia (50% v/v) through a pre-digestion period of 20 min. After this time, digestion was performed in a microwave oven digester with a power of 1600 W and temperature of 175 °C, for 20 min. The final extract was transferred to Falcon tubes and the volume taken to 25 mL with HNO_3 0.2% v/v. The reliability of the analytical results was monitored by means of the simultaneous analysis of certified sediment standard (NIST 1646A) and duplicate analyses of all samples. Standard recovery was higher than 99% for the two elements; the detection limit of the procedure was 0.01 μg g^{-1} for Mn and 0.03 μg g^{-1} for Sr. The content of the metals was quantified using Flame Atomic Absorption Spectrometry - AAS (AA 6200, SHIMADZU). AA calibration was performed through the calibration curves of each metal constructed from MERCK standard solutions (1000 μg g^{-1}).

Isotopes of C (^{13}C and ^{12}C) and O (^{18}O and ^{16}O) concentrations were analyzed in the CO_2 extracted from samples by digestion with orto-phosphoric acid at 25 °C. The $CO_2$was carried to a Thermofinnigan Delta V Advantage mass spectrometer. Results are expressed in the δ notation (‰) with accuracy better than ± 0.1‰. Carbon and oxygen isotopic data were calibrated to international standards (Vienna Pee Dee Belemnite).

There is no general agreement on how to select samples with primary C or O-signals, eliminating those that may have undergone post-depositional change of their isotope values. However, most studies, however, suggest that concentrations of Mn, Sr, Rb and Fe help in selecting samples that have undergone little or no alteration. Among those mostly used to make such an evaluation, Mn/Sr ratios seems more effective, since Sr is preferentially removed during recrystallization of meta-stable carbonate phases, whereas Mn is enriched during formation of late-stage ferroan calcite cement (Kaufman et al., 1993; Kaufman and Knoll, 1995; Jacobsen and Kaufman, 1999). In general, Mn/Sr ratios lower than 10 commonly retain near primary isotopic abundances. A $\delta^{13}C$ and $\delta^{18}O$ cross plots for all formations apparently scatter rather than co-variance seems to predominate. Ratios of Mn to Sr of samples subjected to $\delta^{18}O$ analysis were mostly <10, but varied from 4.6 in the Romualdo Formation (with the exception of a single sample, number 23, with extreme $\delta^{18}O$ of −10.11‰; with Mn/Sr ratios higher than 10), to 4.7 in the Barbalha and Ipubi Formations. In the Crato Formation ratios range from 0.7 to 6.6, but three samples gave values equal or slightly higher than 10, these samples, however, showed Mn and Sr concentrations very close to the detection limit (dl), and therefore were not considered (Table 1). These observations imply that the $\delta^{13}C$ and $\delta^{18}O$ values in most of the samples reported here are primary or near primary values granting a consistent interpretation of the isotopic stratigraphy (Keith and Weber, 1964; Sial et al., 2008).

Corroborating the Mn/Sr results, Fig. 3 shows a graphic plot between $\delta^{13}C$ *vs* $\delta^{18}O$, firstly proposed by Keith and Weber (1964), this type of graph generally separates samples deposited under different environmental conditions, and correct diagnosis is considerably improved in Jurassic and younger samples, such as those from the Araripe Basin reported here (Schobben et al., 2026). The evaluation of potential diagenetic overprints can also be assessed using the diagram, although and $\delta^{13}C$ vs $\delta^{18}O$ covariance depends largely on environmental factors rather than diagenesis, but together with well-calibrated biostratigraphy, recently published by Melo et al. (2020) for the Romualdo Formation and the Mn/Sr ratio already discussed, it is possible to have some control on the C-isotope data. The scattering of $\delta^{13}C$ and $\delta^{18}O$ values presented in Fig. 3, confirms the assessment from the Mn/Sr ratio that the majority of samples fall into the field of weak, if any, diagenesis. The sole exception, as noted in the Mn/Sr ratio is the sample with extreme $\delta^{18}O$ values.

Total organic carbon (TOC) was quantified according to Yeomans and Bremner (1998) in 0.1 g subsamples, digested with 5 mL $K_2Cr_2O_7$ 0.167M solution and 7.5 mL of H_2SO_4 conc., at 170 °C, for 30 min. After cooling in room temperature samples were taken to 80 mL and 3 to 5 drops of ferroin (1.485 g of o-fenatrolin plus 0.695g of ferrous sulfate in 100 mL of deionized water) and titration with $(Fe(NH_4)_2(SO_4)_2)$ 0.2M.

4. Results

Overall TOC concentrations varied from 0.16 to 13.85%, well above concentrations considered unreliable for using it as a proxy of biological productivity and C-org deposition in ancient sediments, thus making the use of the Hg/TOC proxy robust (Grasby et al., 2016; Charbonnier et al., 2017). However, concentrations were different among formations. Highest TOC was found in the Ipubi Formation (3.05%–13.85%), in agreement with highest C-org deposition during this interval, as previously suggested (Assine et al., 2014). Second highest TOC values occurred in the Barbalha Formation (0.30%–3.28%) followed by Ramualdo and Crato Formations (0.16%–1.84% and 0.43–1.42%, respectively) (Table 1). The $\delta^{13}C$ stratigraphy showed negative values in nearly all samples, varying from −11.53 to −0.22‰, but two positive excursions of +0.72‰ in the single sample from the Barbalha Formation and +0.61‰ in the Crato Formation, suggesting intense primary productivity. Unfortunately, due to lack of carbonate layers, in 24 out of 49 samples $\delta^{13}C$ could not be quantified. All $\delta^{18}O$ values were negative varying from −10.11 and −1.17‰.

There are no reported Hg chemostratigraphic analyses in the Araripe Basin deposits. Concentrations reported here are, therefore, the first records of this proxy in this geological setting. Late Albian sediments from the Romualdo Formation showed Hg concentrations varying from 1.11 to 26.33 ng g^{-1}. Both samples from the Ipubi Formation showed relatively high Hg concentrations (8.91 and 20.37 ng g^{-1}). Carbonates from the Crato Formation (Late Aptian – Earlier Albian) showed Hg concentrations varying from 1.37 to 44.04 ng g^{-1} and characterized by four sharp maximum peaks of 34.17 ng g^{-1}, 23.12 ng g^{-1}, 33.75 ng g^{-1} and 44.04 ng g^{-1}.

In the Barbalha Formation, Hg stratigraphy showed concentrations varying from 2.69 to 43.60 ng g^{-1}, with the maximum Hg concentration peak simultaneous to a positive $\delta^{13}C$ excursion (+0.72‰) and a negative $\delta^{18}O$ excursion (−8.65‰) (Fig. 4).

5. Discussion

Between 145 and 50 Ma, global oceans were influenced by numerous environmental changes related to intense pulses of igneous activity associated with the formation of LIPs, which resulted in chemical changes in oceans and atmosphere, increased temperatures, high

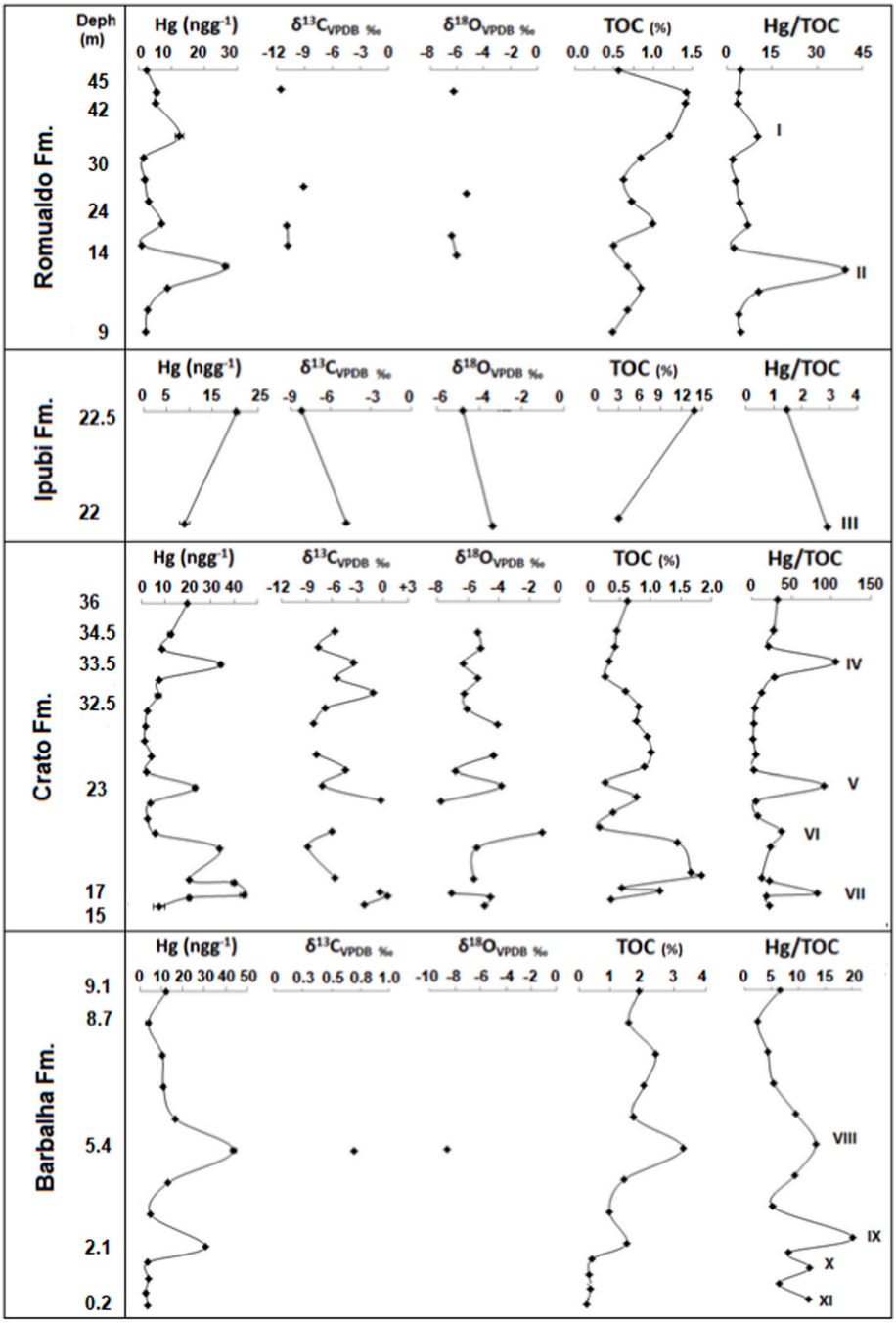

Fig. 4. Concentrations of Hg (ng g^{-1}), C and O isotopes, TOC (%) and Hg/TOC ratio along the studied formations in the Araripe Basin, NE do Brazil.

relative sea level, episodic deposition of black shales, high hydrocarbon production (Coffin et al., 2002). These changes are recorded in the stratigraphic variations in Hg concentration of Hg, $\delta^{13}C$, $\delta^{18}O$ and TOC in the Araripe Basin. LIPs coeval with local and global biotic crises may be due to atmospheric-volcanogenic processes including ocean acidification, metal poisoning, acid rain, ozone damage and consequent increase in UV-B radiation, volcanic darkness, cooling and decreased photosynthesis (Grasby et al., 2015). Volcanic Hg emissions include mostly elemental gaseous (Hg^0), with residence time in the atmosphere from a few months to up to 2 years, allowing its transport away from its source, reaching a regional and even global scale before deposition in terrestrial and marine environments. In the atmosphere, Hg0 is oxidized to reactive Hg^{2+}, soluble in water and therefore enriched in rainwater (Sial et al., 2014, 2016, 2018). As a result, many studies have reported synchronous Hg peaks in the sedimentary record associated with recent (Roos-Barraclough et al., 2002; Lacerda et al., 2017) and prehistoric (Nascimento-Silva et al., 2011; Sanei et al., 2012; Sial et al., 2014) volcanic activities.

The Araripe Basin does not present a record of volcanic activity in the basin, despite this, the Barbalha (113 Ma), Crato (112 Ma), Ipubi (108 Ma) and Romualdo (100 Ma) Formations showed Hg peaks, and these formations may have acted as sedimentary deposit of Hg transported on a regional or even global scale, in their respective periods. It is possible, therefore, that at least some of the Hg peaks found in the above-mentioned formations would be related to volcanic activity external to the Araripe Basin and transported and deposited in sediments in this region. These peaks are coincident with the "superplume" volcanic event in the Middle Cetaceous and the initial Aptian volcanic eruptions

in the Pacific, and this association is supported by the lack of correspondence with any simultaneous peak in TOC distribution.

In a global scale, the occurrence of a volcanic pulse in the Middle Cretaceous caused abnormal formation of the oceanic crust. The phenomenon that occurred in the Pacific Ocean with an abrupt onset would have originated in a super-plume (about 125 Ma), increasing from 50% to 75% the rate of formation of the oceanic crust. This volcanic activity would have caused the creation of several oceanic plateaus in the Pacific and the extrusion of thick and extensive continental flood basalts. Volcanic activity would have started suddenly between 125 and 120 Ma, decreasing its intensity between 120 and 80 Ma. Also, the super-plume event displaced ocean water through underwater volcanic material, which resulted in an eustatic sea-level rise (Phelps et al., 2015), an occurrence observed in the depositional period of the Crato, Ipubi and Romualdo formations in the Albian. This event has produced an excess CO_2in the atmosphere, accelerating the hydrological cycle and resulting in increasing continental runoff and weathering, augmenting sediment, nutrients and trace elements transfer to the sea and eventually inducing bio-calcification crises (Phelps et al., 2015; Sabatino et al., 2018).

Between the Late Aptian and the Early Albian there were significant changes in the carbon cycle associate with an OAE connected to the Kerguelen volcanism, but the lack of precise ages prevents a correlation with the mentioned events. A section in the Poggio le Guaine, Umbria-Marche Basin in Italy displays anomalous Hg concentrations during this interval. The Hg enrichment was associated with increasing Hg emissions from volcanism of the major phase of the Kerguelen LIP (Sabatino et al., 2018).The explosive nature of the Kerguelen volcanism would have ejected Hg-enriched particles and gaseous Hg to the stratosphere, allowing its global distribution (Coffin et al., 2002). The Kerguelen Oceanic Plateau in the South Indian Ocean is the world second largest and is operationally classified in five distinct dominions: the South Kerguelen Plateau (SKP) (~119-110 Ma), the Central Kerguelen Plateau (CKP) (~103-95 Ma), the North Kerguelen Plateau (NKP), Elan Bank (~114–109.5 Ma) and Broken Ridge (89.2–88 Ma) (Coffin et al., 2002; Frey et al., 2002; Courtillot and Renne, 2003).The observed Hg spikes from the Poggio le Guaine section coeval with some formations of the Araripe Basin, which are also characterized by Hg spikes unassociated with TOC distribution, suggesting distal volcanic emissions as the likely origin of the Hg spikes, that are linked to Kerguelen volcanism. The negative δ^{13}Cexcursions also suggest significant environmental changes.

Regionally intensive volcanism in South America occurred in the Creataceous attested by the basalts of the immense Serra Geral Formation, one of the largest in the planet. However, the largest lava production took place between 134.5 Ma and 129 Ma (Pinto et al., 2011), therefore, hardly affecting the Araripe Basin geochemistry.

The high affinity of Hg to organic matter allows an interpretation of the importance of internal process on Hg concentration in sedimentary profiles through the Hg/TOC ratio (Gehrke et al., 2009). Once in the marine environment Hg can be incorporated by plankton and/or absorbed onto suspended particles, both scavenge Hg to bottom sediments where deposition and further burial occur. In most open water environments organic matter dominates over clay particles, which normally deposit close to fluvial sources (Lacerda et al., 2020). Thus Hg/TOC ratios can be used as a proxy of environmental conditions and external sources of Hg to sediments (Sanei et al., 2012; Grasby et al., 2013, 2016; Font et al., 2016; Charbonnier et al., 2017).

Various studies have also observed discrete peaks in the Hg/TOC ratios in the sedimentary record, in particular the Cretaceous-Paleogene boundary around the world, when dinosaurs became extinct, among other groups (see Sial et al., 2018) for a recent, comprehensive review). These peaks were associated with the Deccan volcanism and have intensified the debate on impact vs volcanism as the major cause of dinosaur extinctions (Font et al., 2016). Other boundaries coeval to biological crises seems to present similar results. In the Sverdrup Basin (Arctic Canada), Hg/TOC ratios were used to characterize changes in biogeochemical cycles during the Permian-Triassic biological crises. The ratios showed a strong co-variation between Hg and TOC, but a large Hg/TOC peak occurs in the at the end of the Permian, suggesting an anomalous event resulting in an extra-large load of Hg to the environment, in this case associated with the Siberian Traps volcanism. During most of the Permian-Triassic transition, Hg/TOC ratios were relatively constant suggesting an oceanic baseline for the period (Grasby et al., 2013).

In the Araripe samples Hg concentrations showed no significant correlation ($n = 49$, $p > 0.05$) with TOC. Although there is no clear indication that sedimentary deposition of formations in the Araripe Basin occurred concomitantly with volcanic activity, concentrations of Hg that deviated from the linear Hg/TOC relationship, suggests an external source of Hg to the basin, such as volcanism. Emissions could reach the basin either through direct atmospheric deposition and/or through connections with distal sites by transgressions of seas enriched in Hg.

The Middle Cretaceous (about 120 to 80 Ma) was considered a period of enhanced greenhouse effect, with high atmospheric concentrations of CO_2, high global average temperatures (Larson and Erba, 1999; Wilson and Norris, 2001) and a series of ocean anoxic events (OAE) that promoted the widespread deposition of marine sediments rich in organic carbon and significant biological changes. Global stratigraphic data highlights that average sea levels throughout the Cretaceous remained ~75–250 m higher than present day mean sea level (PDMSL). Haq (2014) showed a relatively high and stable sea level in the Aptian to the Albian, with variation of only ~15 m, but followed by a rapid increase to a maximum of ~205–215 m above PDMSL.

Müller et al. (2008) made a comprehensive reconstruction of the temporal variability of the area and the relationship between area and depth of the ocean bottom, including the remaining subducted crust, in the last 140 Ma. This reconstruction also considered the effects of changes in continental crust production, sediment inputs, and the location and intensity of LIPs, factors that would have resulted in a total sea level increase by almost 100 m since 140 Ma, with larger pulses at about 120, 110, 90, 60 and 40 Ma, suggesting a sea level at the end of the Upper Cretaceous of about 170 m (85–270 m) relative to PDMSL. In addition, they have estimated a total sea level increase of about 70 m between 140 and 110 Ma, causing continental flooding in the Cretaceous. When considering the effect of LIPs in the Albian stage, the authors highlight the influence of the Kerguelen plateau.

The Kerguelen LIP represented a continuous process that began with the dismemberment of Gondwana and the formation of the Kerguelen plateau in the Cretaceous (Borisova et al., 2014; Olierook et al., 2019). Among the various phases of volcanic activity, Elan Bank, a western microcontinent of Kerguelen that originally stood between India and Antarctica in Gondwana, had its basaltic volcanism occurred around 109 Ma (Ingle et al., 2002). The Aptian-Albian interval in the Araripe Basin was therefore influenced by the global climatic conditions prevailing during the Cretaceous period, including a warm and highly saline ocean with regressive-transgressive cycles that lasted approximately 1–3 Ma (Fambriniet al., 2019). It is thus possible, that part of the observed Hg peaks recorded in the Araripe Basin could have originated during independent on the location of its origin in the Atlantic Ocean (Martill et al., 2007; Heimhofer et al., 2008).The first marine transgression in the Araripe Basin occurred in the Late Albian, dated at 104.2 Ma and resulted in the shale deposition in the Ipubi formation. This formation is represented by a siliciclastic-evaporitic succession, representing the phase I post-rift, a shallow marine-lacustrine environment. A subsequent transgression would have caused the deposition of siliciclastic rocks of the Romualdo Formation on top of the strata of the Ipubi Formation, and also promoted a new event of karst formation of the upper evaporite beds of the Ipubi (Fabin et al., 2018).

The Romualdo Formation shows clear evidence of a paleoenvironment with marine transgressions or marine transition areas (Valença et al., 2003; Santana et al., 2013; Melo et al., 2020), suggested by the

abundant occurrence of fossils of marine organisms (Assine et al., 2014; Kellner, 2002; Pinheiro et al., 2014) and strengthening the idea that the Romualdo Formation deposited under some degree of salinity and although a relatively isolated region from the sea, the latter could have flooded the basin sporadically (Santana et al., 2013). The Kerguelen LIP activity may have been the main trigger of eustatic marine transgressions in the Araripe Basin. The Aptian-Albian was a phase marked by an intense nutrient cycle coupled to an accelerated global hydrological cycle resulting from an increase in atmospheric CO_2. During this period Pangea experienced a process of accelerated disintegration, resulting in an enlargement of the seabed, associated with the onset of volcanic activity in the Pacific (Weissert, 1989). Most of these environmental changes are registered as changes in the $\delta^{13}C$ and $\delta^{18}O$composition of carbonates that varied among the different formations of the Araripe Basin.

Carbon isotope stratigraphy in the Barbalha Formation, although represented by only one value ($\delta^{13}C$ +0.72‰ VPDB), in a sample with the highest recorded TOC content (3%), suggests a high bioproductivity and represents the registration of the onset of the first lake system in the basin (Assine, 2007). The simultaneous $\delta^{18}O$ record (−8.65‰ VPDB) also suggests a warm period influenced by high precipitation. Up the stratigraphic column, at the beginning of Albian in the Crato Formation, $\delta^{13}C$ was mostly negative (−8.90 to +0.61‰ VPDB) and suggests a fresh water environment possibly formed through the contribution of meteoric water and/or with the contribution of CO_2 from the mantle. The three positive excursions in the $\delta^{13}C$ profile represent repeated cycles of an environment that suffered gradual deterioration of organic productivity, followed by its recovery or more saline lagoon environment at the most positive points. The mostly negative $\delta^{18}O$ profile of the Crato Formation also presented repeated positive and negative oscillations, suggesting gradual temperature fluctuations and changes in the lake level, as well as the existence of fresh water during carbonate precipitation. A similar scenario was suggested base on Aptian lacustrine carbonates of Serra do Tonã, Tucano Norte Basin also in NE do Brazil, that showed $\delta^{13}C$ varying from −8.76 to 1.41‰ VPDB and $\delta^{18}O$ from −14.28 to −4.14‰ VPDB, characterizing a close lacustrine system with fresh water in the base and more saline waters in intermediary layers. These laminated carbonates are morphological very similar to those of the Crato Formation (Silveira et al., 2014).

The negative $\delta^{13}C$ excursions (−4.81 to −8.15‰ VPDB) and $\delta^{18}O$ (−3.40 to −4.77‰ VPDB) in the pyrobituminous shale of the Ipubi Formation in addition to high TOC (3.05–13.85%) are typical of an anoxic environment and displaying high preservation of C-org. The bituminous black shales of the Ipubi Formation may contain up to 25% TOC, a consequence of the transgressive pulse caused by a relative increase in the level of the lake (Fabin et al., 2018). The $\delta^{18}O$ values in sulfates of this formation, varied between +7.72‰ and +13.30‰, suggesting a marine environment with its evaporites deposited in a subaqueous context (saline) and intra sediment in a coastal sabkha, which explains the enrichment of Hg in these sediments whose maximum peaks disappear when normalized by TOC (Bobco et al., 2017).

In the Late Albian Romualdo Formation, the TOC curve, partially corroborated by the small number of $\delta^{13}C$, suggests increasing primary productivity under more arid conditions and possible marine deposition, suggested by the dense coquinoid layer, including rich fossils of ostracods, mollusks and equinoderms of typical marine origin present in this section (Maisey and Carvalho, 1995; Assine, 2007). Most $\delta^{18}O$ values are negative throughout, the most negative value at the top (−10.11‰ VPDB) of the section, a value not typical of marine carbonates that may represent a diagenetic overprint of oxygen isotopes. In fact Mn/Sr ratio of this sample is slightly higher than 10, also suggesting some overprint. Positive excursions of $\delta^{13}C$ may also suggest the occurrence of an episode coupling changes in the global carbon cycle and the submersion of the continental shelf, as a consequence of enhanced greenhouse conditions, which may have been triggered by episodes of extensive volcanism (Föllmi et al., 1994). In this scenario, the Romualdo Formation was a submersed area with marine influence with prevailing increase in biological productivity in an environment with warmer temperatures and increased precipitation in the more recent layers.

The negative shift of $\delta^{13}C$, recurrent in several crises related to smaller biological productivity may result from the introduction of large amounts of CO_2 into the atmosphere through intense volcanism, which in many cases are coeval with LIPs (Pálfy et al., 2001). In this context extrinsic mechanisms related to the presence of important episodes of volcanism in the Cretaceous, such as the Kerguelen Plateau may have induced climatic, oceanographic and environmental changes in a global context which caused disturbances in the Araripe Basin environment.

Among mechanisms associated with the Kerguelen LIP, OAEs result from profound changes in the global ocean state and major disturbances in the global carbon cycle. Although the triggering mechanism of these events is not fully understood, OAEs may result from an abrupt increase in temperature, induced by the rapid influx of CO_2 into the atmosphere from volcanogenic and/or methanogenic sources (Phelps et al., 2015). OAEs are recorded by the anomalous occurrence of black shale units rich in organic carbon, deposited under poorly oxygenated conditions evolving to anoxic and finally euxinic (sulfidic) conditions (Jenkyns, 2010).

Numerous extinction events appear well associated with most OAEs during the Jurassic-Cretaceous, including the beginning of the Toartian (Posidonienschiefer event, T-OAE, ‘183 Ma), Early Aptian (Selli event, OAE 1a, ‘120 Ma), Albian (Paquier event, OAE 1b, ‘111 Ma), Late Albian (OAE c, OAE 1d) and Cenomanian-Turonian (Bonarelli event, C/T OAE, OAE 2, ‘93 Ma) (Jenkyns, 2010). Transgression during the compound sequence of the Early Aptian (124-119 Ma) and the effects of OAE 1a appear related to underwater volcanism in the Ontong-Java Plateau that coincided with an eustatic increase in the global stratigraphic records. Immediately after EOA 1a, the platform’s second submersion event and the start of shale deposition began with the Fallot Event and continued during the Paquier event of the OAE 1b set. The Fallot event and the OAE 1b set were preceded by long-term negative trends for $\delta^{13}C$ in several segments. Similar to what occurred in OAE 1a, the eustatic increase in the Late Aptian composite sequence (119-110 Ma) and the negative $\delta^{13}C$ values were coincident with the volcanism of igneous province in the Nauru-Mariana Basin and the Kerguelen Plateau (Weissert and Erba, 2004; Phelps et al., 2014, 2015).

Heimhofer et al. (2008) point out that the deposition of pyrobituminous shales in the Araripe Basin was related to an overall eustatic increase in sea-level. The authors proposed three different scenarios to explain the intensified accumulation C-org in the Araripe Basin; (1) coastal erosion as a direct response to sea level rise and nutrient leaching during a transgressive event, leading to increased fertilization of surface waters and increased productivity in basin waters; (2) a circulatory pattern associated with thermohaline stratification, where increased productivity would have been triggered by high streams of riverside nutrients and, in combination with salinity-controlled surface water stratification and limited vertical mixing, resulting in oxygen deficiency conditions within the water column and at the bottom of the sea; (3) intrusion of anoxic (or oxygen deficient) waters from the evolving Atlantic Ocean.

The Crato Formation that precedes the Ipubi Formation in the stratigraphic profile of the Araripe Basin, characterized by thick carbonate sequences, has been considered as a saline lacustrine depositional unit with eventual intrusion of fresh water (Bruno and Hessel, 2006) and may have its sedimentation interrupted as an antecedent phenomenon of OAE 1b that may have influenced the Ipubi Formation. In a study by Phelps et al. (2015) it was highlighted that on four separate occasions, low-amplitude eustatic sea level rise and environmental disturbances involving ocean anoxic events 1a, 1b, 1d and 2 interrupted carbonate deposition on the Comanche Platform (northern Gulf of Mexico), with shale deposition accompanied or immediately at each episode of flooding on the platform.

The major drivers of the environmental changes that occurred in the

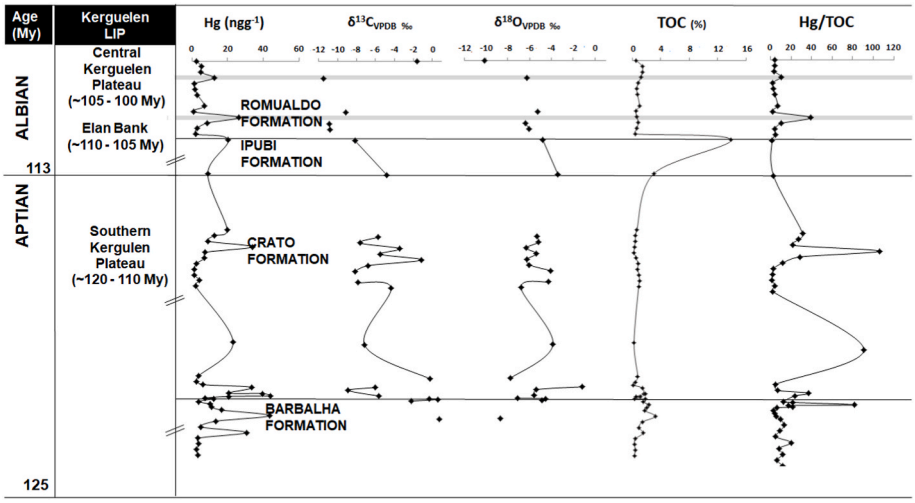

Fig. 5. Concentrations of Hg, C and O isotopes, total organic carbon (TOC) isotopes in line with different periods of the Kerguelen LIP activity following Coffin et al. (2002). Shaded areas represent ate biological crisis.

Aptian-Albian stage that led to the extinction of species in the Araripe Basin, volcanism and OAEs, are suggested by the stratigraphy of Hg and isotopes of C and O. Among them, volcanism has already been suggested as one of the main causes of intense biological crises (Font et al., 2016; Benigno et al., 2018). Fig. 5 presents the stratigraphic profile of Hg, $\delta^{13}C$, $\delta^{18}O$, TOC and the Hg/TOC ratios, relating them to the period of activity of the Kerguelen LIP that may have influenced the occurrence of biological disturbances in the Araripe Basin. The Hg peaks observed in the Crato and Romualdo Formations show independence from TOC variations, strongly suggesting the influence of volcanism on the basin and in local biological crises. At least for the Romualdo Formation, recent work (Saraiva et al., 2007) of the intensity of fish mortality places peaks of mortality coincident with Hg/TOC positive excursions I and II shown in Fig. 4, which are coeval with the Central Kerguelen Plateau volcanic activity. However, one has to take into consideration the scarcity of quantitative data on the fossil record of the Araripe Basin; therefore the association between distal volcanism and biological crises is still debatable. It is known that strong negative excursions of $\delta^{13}C$ in marine carbonates generally appear related to periods of mass extinctions (Kump, 1991), which implies that biotic crises are associated with changes in the global carbon cycle (Pálfy et al., 2001). Keller (2008) complements and argues relating biotic crises to generalized OAEs accompanied by changes in sea level and climate change, such as those in the Aptian-Albian, leading to high stressful conditions to the biota, largely due to high levels of nutrients associated with heating, increased weather extremes and the onset of LIPs. In the Ipubi Formation, OAEs may have played a most significant role as driver of local biological crises. Although expansive seas have provided new habitats for marine and terrestrial life from shallow waters, leading to diversification, they can be considered a potentially critical influence on extinctions. For rapid regressions can seriously decrease the space of the marine ecosystem, leading to marine extinction as observed in several Faneroozoic extinctions (Kidder and Worsley, 2010).

6. Conclusions

Along the stratigraphic profile covering the four main formations of the Araripe Basin we observed the existence of high Hg concentration peaks in some of the analyzed samples not associated with an increase in TOC deposition. This result corroborates the hypothesis that volcanism possibly influenced changes in oceanic and climatic conditions that led, at least in part, to the death of fauna and flora in the Araripe Basin, particularly in the Romualdo and Crato Formations. Although dating is still limited, the major period of Kerguelen LIP volcanism is coeval with Hg peaks in the mentioned formations. TOC-independent Hg anomalies strongly suggest a direct action of volcanism, as reported in other sites during the Cretaceous. In the Ipubi formation, however, impact of volcanism is uncertain and cannot be separated from background processes and/or cumulative environmental changes, suggested by the strong relationship between Hg and TOC, a possible result of increasing C-org deposition and OAE conditions in the basin. It is possible, therefore, to correlate the contribution of Kerguelen's volcanism to paleoenvironmental stress in the Araripe Basin, which would have caused environmental disturbances and directly and indirectly resulted in biological crises denounced by the fossil record.

Author statement

Ana Paula Benigno: Methodology, investigation, visualization and writing the original draft; Luiz D. Lacerda: Project administration, conceptualization, investigation, resources, writing the original draft and review and editing, Antônio A.S. Feitosa: Visualization, methodology, investigation, resources, reviewing and editing. Alcides N. Sial: Supervision, methodology investigation, resources and review and editing. This manuscript has not been submitted previously to any other journal. All authors subscribe and agree with the submitted materials.

Funding

This study was funded by the Fundação Cearense de Apoio ao Desenvolvimento Científico e Tecnológico (FUNCAP), Proc. No.INT-0159-00009.01.00/19 and grants to L.D. Lacerda from the Brazilian Council for Scientific and Technological Development (CNPq), Proc. No.405.244/2018-5.

Declaration of competing interest

The authors declare that they have no known competing financial interests or personal relationships that could have appeared to influence the work reported in this paper.

Acknowledgments

The authors are deeply indebted to the many students of the Regional University of Cariri who has helped in the intensive field campaigns in the Araripe Basin. Technicians from the Marine Biogeochemistry Laboratory (LBC-UFC) helped prepare samples for chemical analyses, whereas those from the NABISE-UFPE, for isotopes analysis. Our special

thanks are due to 2 anonymous reviewers who greatly improve earlier versions of this manuscript.

References

Aguiar, J.E., Marins, R.V., Almeida, M.D., 2007. Comparação de metodologias de digestão de sedimentos marinhos para caracterização da geoquímica de metais-traço na plataforma continental nordeste oriental brasileira. Geochim. Bras. 21, 304–323.

Assine, M.L., 1992. Análise Estratigráfica da Bacia do Araripe, Nordeste do Brasil. Rev. Bras. Geociencias 22, 289–300.

Assine, M.L., 1994. Paleocorrentes e paleogeografia na Bacia do Araripe, nordeste do Brasil. Rev. Bras. Geociencias 24, 223–232.

Assine, M.L., 2007. Bacia do Araripe. Bol. Geociencias Petrobras 15, 371–389.

Assine, M.L., Perinotto, J.A.J., Custódio, M.A., Neumann, V.H., Varejão, F.G., Mescolotti, P.C., 2014. Sequências deposicionais do Andar Alagoas da Bacia do Araripe, Nordeste do Brasil. Bol. Geociencias Petrobras 22, 3–28.

Barbosa, J.A., Hessel, M.H., Neumann, V.H., 2004. Bivalves da Formação Crato, Bacia do Araripe. Paleontol. Destaque 20, 41–42.

Barros, O.A., Pinheiro, A.P., Batista, E.P., Silva, J.H., Saraiva, A.A.F., 2016. Aspectos paleoecológicos da macrofauna dos folhelhos associados à camada de gipsita, Bacia do Araripe. Est. Geol. UFPE 26, 147–156.

Benigno, A.P.A., Sial, A.N., Lacerda, L.D., 2018. Estratigrafia de Hg como traçador de vulcanismo e crises biológicas na transição Cretáceo-Paleogeno. Rev. Virtual Quím. 10, 655–671.

Bobco, F.E.R., Goldberg, K., Bardola, T.P., 2017. Modelo deposicional do Membro Ipubi (Bacia do Araripe, nordeste do Brasil) a partir da caracterização faciológica, petrográfica e isotópica dos evaporitos. Pesqu. Geociênc. 44, 431–451.

Bond, D.P.G., Wignall, P.B., 2014. Large igneous provinces and mass extinctions: an update. In: Keller, G., Kerr, A.C. (Eds.), Volcanism, Impacts, and Mass Extinctions: Causes and Effects. Geol. Soc. Am. Spec. Pap., vol. 505, pp. 29–55.

Borisova, A.Y., Faure, F., Deloule, E., Grégoire, M., Béjina, F., Parseval, P., Devidal, J.-L., 2014. Lead isotope signatures of Kerguelen plume-derived olivine-hosted melt inclusions: constraints on the ocean island basalt petrogenesis. Lithos 198–199, 153–171.

Bralower, T.J., Arthur, M.A., Leckie, R.M., Sliter, W.V., Allard, D.J., Schlanger, S.O., 1994. Timing and paleoceanography of oceanic dysoxia/anoxia in the late barremian to early aptian (early cretaceous). Palaios 9, 335–369.

Bralower, T.J., Cobabe, E., Clement, B., Sliter, W.V., Osburn, C.L., Longoria, J., 1999. The record of global change in mid-Cretaceous (Barremian-Albian) sections from the Sierra Madre, northeastern Mexico. J. Foraminifer. Res. 29, 418–437.

Bruno, A.P.S., Hessel, M.H., 2006. Registros paleontológicos do Cretáceo marinho na Bacia do Araripe. Est. Geol.UFPE 16, 30–49.

Camacho, C.R., Oliveira e Sousa, F.R.F.R., 2017. O arcabouço estrutural da Bacia Sedimentar do Araripe, Província Borborema, baseado em dados aeromagnetométricos. Rev. Inst. Geociênc. USP Sér. Cient. 17, 114–161.

Carmo, D.A., Rafael, R.M.L., Vilhena, R.M., Tomassi, H.Z., 2004. Redescrição de *Theriosynoecum silvai eDarwinula martinsi*, membroCrato (Formação Santana), Cretáceoinferior, Bacia do Araripe, NE, Brasil. Rev. Bras. Palaontol. 7, 151–158.

Castro, J.C., Valença, L.M.M., Neumann, V.H., 2006. Ciclos e sequências deposicionais das formações Rio da Batateira e Santana (andar Alagoas), Bacia do Araripe, Brasil. Geociencias 25, 289–296.

Ceará State Goverrmment, 2012. Araripe: Geopark Stories of a Land, a Culture and an Environment. State Government Ceará, Department of Municipalities, Ceará Cities Project - Cariri Central – Crato, Fortaleza, p. 167.

Chagas, D.B., Assine, M.L., Freitas, F.I., 2007. Sedimentary facies and depositional environments of the Barbalha Formation, Araripe basin, northeastern Brazil. Geociencias 26, 313–322.

Charbonnier, G., Morales, C., Duchamp-Alphonse, S., Westermann, S., Adatte, T., Föllmi, K.B., 2017. Mercury enrichment indicates volcanic triggering of Valanginian environmental change. Sci. Rep. 7, 40808.

Coffin, M.F., Pringle, M.S., Ducan, R.A., Gladczenko, T.P., Storey, M., Müller, R.D., Gahagan, L.A., 2002. Kerguelen hotspot magma output since 130 Ma. J. Petrol. 43, 1121–1137.

Coimbra, J.C., Arai, M., Carreño, A.L., 2002a. Biostratigraphy of lower cretaceous microfossils from the Araripe Basin, northeastern Brazil. Geobios 35, 687–698.

Coimbra, J.C., Arai, M., Carreño, A.L., 2002b. Biostratigraphy of lower cretaceous microfossils from the Araripe basin, northeastern Brazil. Geobios 35, 687–698. https://doi.org/10.1016/S0016-6995(02)00082-7.

Costa, A.B.S., Córdoba, V.C., Sá, E.F.J., Scherer, C.M.S., 2014. Diagênese dos arenitos da tecnossequência rifte na Bacia do Araripe, NE do Brasil. Braz. J. Genet. 44, 457–470.

Courtillot, V.E., Renne, P.R., 2003. On the ages of flood basalt events. Compt. Rendus Geosci. 335, 113–140.

Fabin, C.E., Correia Filho, O.J., Alencar, M.L., Barbosa, J.A., Miranda, T.S., Neumann, V. H., Gomes, I.F., Santana, F.R., 2018. Stratigraphic relations of the Ipubi formation: siliciclastic-evaporitic succession of the Araripe basin. An. Acad. Bras. Ciênc. 90, 2049–2071.

Fambrini, G.L., Lemos, D.R., Tesser Jr., S., Araújo, J.T., Silva-Filho, W.F., Souza, B.Y.C., Neumann, V.H.M., 2011. Estratigrafia, arquitetura deposicional e faciologia da Formação Missão Velha (Neojurássico-Eocretáceo) na área-tipo, Bacia do Araripe, Nordeste do Brasil: exemplo de sedimentação de estágio de início de rifte a clímax de rifte. Rev. Inst. Geociênc. USP 11, 55–87.

Fambrini, G.L., Neumann, V.H., Silva-Filho, W.F., Menezes-Filho, J.A.B., Tesser Junior, S., Araújo, J.T., Lemos, D.R., Silvestre, D.C., 2019. Análise tectonossedimentar das fases início de rifte e clímax de rifte da Bacia do Araripe, Nordeste do Brasil. Geol. Usp. Série Científica 19, 205–236.

Fara, E., Saraiva, A.A.F., Campos, D.A., Moreira, J.K.R., Siebra, D.C., Kellner, A.W.A., 2005. Controlled excavations in the Romualdo member of the Santana formation (early cretaceous, Araripe basin, northeastern Brazil): stratigraphic, palaeoenvironmental and palaeoecological implications. Palaeogeogr. Palaeoclimatol. Palaeoecol. 218, 145–160.

Föllmi, K.B., Weissert, H., Bisping, M., Funk, H., 1994. Phosphogenesis, carbon-isotope stratigraphy, and carbonate-platform evolution along the Lower Cretaceous northern Tethyan margin. Geol. Soc. Am. Bull. 106, 729–746.

Font, E., Adatte, T., Sial, A.N., Lacerda, L.D., Keller, G., Punekar, J., 2016. Mercury anomaly, Deccan volcanism and the end-Cretaceous mass extinction. Geol. 44, 171–174.

Frey, F.A., Weis, D., Borisova, A.Y., Xu, G., 2002. Involvement of continental crust in the formation of the cretaceous Kerguelen plateau: new perspectives from ODP leg 120 sites. J. Petrol. 43, 1207–1239.

Gehrke, G.E., Blum, J.D., Meyers, P.A., 2009. The geochemical behaviour and isotopic composition of Hg in a mid-Pleistocene western Mediterranean sapropel. Geochem. Cosmochim. Acta 73, 1651–1665.

Grasby, S.E., Sanei, H., Beauchamp, B., Chen, Z., 2013. Mercury deposition through the Permo-Triassic biotic crisis. Chem. Geol. 351, 209–216.

Grasby, S.E., Beauchamp, B., Bond, D.P.G., Wignall, P., Talavera, C., Galloway, J.M., Piepjohn, K., Reinhardt, L., Blomeier, D., 2015. Progressive environmental deterioration in northwestern Pangea leading to the latest Permian extinction. Geol. Soc. Am. Bull. 127, 1331–1347.

Grasby, S.E., Beauchamp, B., Bond, D.P.G., Wignall, P.B., Sanei, H., 2016. Mercury anomalies associated with three extinction events (capitanian crisis, latest permian extinction and the smithian/spathian extinction) in NW Pangea. Geol. Mag. 153, 285–297.

Haq, B.U., 2014. Cretaceous eustasy revisited. Global Planet. Change 113, 44–58.

Heimhofer, U., Hesselbo, S.P., Pancost, R.D., Martill, D.M., Hochuli, P.A., Guzzo, J.V.P., 2008. Evidence for photic-zone euxinia in the early albian Santana formation (Araripe basin, NE Brazil). Terra. Nova 20, 347–354.

Ingle, S., Weis, D., Scoates, J.S., Frey, F.A., 2002. Relationship between the early Kerguelen plume and continental flood basalts of the paleo-Eastern Gondwanan margins. Earth Planet Sci. Lett. 197, 35–50.

Jacobsen, S.B., Kaufman, A.J., 1999. The Sr, C and O isotopic evolution of Neoproterozoic seawater. Chem. Geol. 161, 37–57.

Jenkyns, H.C., 2010. Geochemistry of oceanic anoxic events. G-cubed 11, Q03004. https://doi.org/10.1029/2009GC002788.

Kaufman, A.J., Knoll, A.H., 1995. Neoproterozoic variations in the C-isotopic composition of seawater: stratigraphic and biogeochemical implications. Precambrian Res. 73, 27–49.

Kaufman, A.J., Jacobsen, S.B., Knoll, A.H., 1993. The Vendian record of Sr- and C-isotopic variations in seawater: implications for tectonics and paleoclimate. Earth Planet Sci. Lett. 120, 409–430.

Keith, M.L., Weber, J.N., 1964. Carbon and oxygen isotopic composition of selected limestones and fossils. Geochim. Cosmochem. Acta 28, 1787–1816.

Keller, G., 2008. Cretaceous climate, volcanism, impacts and biotic effects. Cretac. Res. 29, 754–771.

Kellner, A.W.A., 2002. Membro Romualdo da Formação Santana, Chapada do Araripe, CE. Um dos mais importantes depósitos fossilíferos do Cretáceo brasileiro. In: Schobbenhaus, C., Campos, D.A.C., Queiroz, E.T., Winge, M., Berbert-Bron, M., Org (Eds.), Sítios geológicos e paleontológicos do Brasil. Brasília, Departamento Nacional da Produção Mineral, vol. 1, pp. 121–130.

Kidder, D.L., Worsley, T.R., 2010. Phanerozoic large igneous provinces (LIPs), HEATT (haline euxinic acidic thermal transgression) episodes, and mass extinctions. Palaeogeogr. Palaeoclimatol. Palaeoecol. 295, 162–191.

Kump, L.R., 1991. Interpreting carbono-isotope excursions: strangelove oceans. Geol. 19, 299–302.

Lacerda, L.D., Turcq, B., Sifeddine, A., Cordeiro, R.C., 2017. Mercury accumulation rates in Caço Lake, NE Brazil during the past 20.000 years. J. South Am. Earth Sci. 77, 42–50.

Lacerda, L.D., Marins, R.V., Dias, F.J.S., 2020. An Arctic paradox: response of fluvial hg inputs and bioavailability to global climate change in an extreme coastal environment. Front. Earth Sci. 8, 1–12. https://www.frontiersin.org/articles/10.3389/feart.2020.00093/full.

Larson, R.L., Erba, E., 1999. Onset of the Mid-Cretaceous greenhouse in the Barremian-Aptian: igneous events and the biological, sedimentary, and geochemical responses. Paleoceanography 14, 663–678.

Maisey, J.G., Carvalho, M.G.P., 1995. First records of fossil Sergestid decapods and fossil brachyuran crab larvae (Arthropoda, Crustacea), with remarks on some Palaemonid fossils from Santana Formation (Aptian-Albian, NE Brazil). Am. Mus. Novit. 3132, 1–20.

Martill, D., Bechly, G., Loveridge, R., 2007. The Crato Fossil Beds of Brazil: Window into an Ancient World. Cambridge University Press, Cambridge.

Melo, R.M., Guzmán, J., Almeida-Lima, D., Piovesan, E.K., Newmann, V.H.M.L., Sousa, A.J., 2020. New marine data and age accuracy of the Romualdo formation, Araripe basin, Brazil. Sci. Rep. 10, 15779. https://doi.org/10.1038/s41598-020-72789-8.

Mochiutti, N.F., Guimarães, G.B., Moreira, J.C., Lima, F.F., Freitas, F.I., 2012. Os valores da geodiversidade: geossítios do Geopark Araripe/CE. An. Inst. Geociênc. UFRJ 35, 173–189.

Müller, R.D., Sdrolias, M., Gaina, C., Steinberger, B., Heine, C., 2008. Long-term sea-level fluctuations driven by ocean basin dynamics. Science 319, 1357–1362.

Nascimento-Silva, M.V., Sial, A.N., Ferreira, V.P., Neumann, V.H., Barbosa, J.A., Pimentel, M.M., Lacerda, L.D., 2011. Cretaceous-Paleogene transition at the Paraiba

Basin, Northeastern, Brazil: carbon-isotope and mercury subsurface stratigraphies. J. South Am. Earth Sci. 32, 379–392.
Neumann, V.H., Gale, J., Reed, R.M., Barbosa, J.A., 2008. Padrão de fraturamento nos calcários laminados Aptianos da região de Nova Olinda-Santana do Cariri, Bacia do Araripe: uma aplicação da técnica de escalas. Est. Geol. UFPE 18, 101–116.
Olierook, H.K.H., Jiang, Q., Jourdan, F., Chiaradia, M., 2019. Greater Kerguelen large igneous province reveals no role for Kerguelen mantle plume in the continental breakup of eastern Gondwana. Earth Planet Sci. Lett. 511, 244–255.
Pálfy, J., Demény, A., Haas, J., Hetényi, M., Orchard, M.J., Vetö, I., 2001. Carbon isotope anomaly and other geochemical changes at the Triassic-Jurassic boundary from a marine section in Hungary. Geol. 29, 1047–1050.
Paula Freitas, A.B.L., Borghi, L., 2011. Estratigrafia de alta resolução do intervalo siliciclástico Aptiano da Bacia do Araripe. Geociencias 30, 529–543.
Percival, L.M.E., Witt, M.L.I., Mather, T.A., Hermoso, M., Jenkyns, H.C., Hesselbo, S.P., Al-Suwaidi, A.H., Storm, M.S., Xu, W., Ruhl, M., 2015. Globally enhanced mercury deposition during the end-Pliensbachian extinction and Toarcian OAE: a link to the Karoo-Ferrar Large Igneous Province. Earth Planet Sci. Lett. 428, 267–280.
Percival, L.M.E., Ruhl, M., Hesselbo, S.P., Jenkyns, H.C., Mather, T.A., Whiteside, J.H., 2017. Mercury evidence for pulsed volcanism during the end-Triassic mass extinction. Proc. Natl. Acad. Sci. Unit. States Am. 114, 7929–7934.
Phelps, R.M., Kerans, C., Loucks, R.G., Da Gama, R.O.B.P., Jeremiah, J., Hull, D., 2014. Oceanographic and eustatic control of carbonate platform evolution and sequence stratigraphy on the Cretaceous (Valanginian-Campanian) passive margin, northern Gulf of Mexico. Sedimentology 61, 461–496.
Phelps, R.M., Kerans, C., Da-Gama, R.O.B.P., Jeremiah, J., Hull, D., Loucks, R.G., 2015. Response and recovery of the Comanche carbonate platform surrounding multiple Cretaceous oceanic anoxic events, northern Gulf of Mexico. Cretac. Res. 54, 117–144.
Pinheiro, A.P., Saraiva, A.A.F., Santana, W., 2014. Shrimps from the Santana group (cretaceous: albian): new species (Crustacea: Decapoda: dendrobranchiata) and new record (Crustacea: Decapoda: caridea). An. Acad. Bras. Ciênc. 86, 663–670.
Pinto, V.M., Hartmann, L.A., Santos, J.O.S., Mcnaughton, N.J., Wildner, W., 2011. Zircon U–Pb geochronology from the Paraná bimodal volcanic province support a brief eruptive cycle at ~135 Ma. Chem. Geol. 281, 93–102.
Rios-Netto, A.M., Regali, M.S.P., Carvalho, I.S., Freitas, F.I., 2012. Palinoestratigrafia do intervalo Alagoas da Bacia do Araripe, Nordeste do Brasil. Rev. Bras. Geocien. 42, 331–342.
Roos-Barraclough, F., Martinez-Cortizas, A., Garca-Rodeja, E., Shotyk, W., 2002. A 14,500 year record of the accumulation of atmospheric mercury in peat: volcanic signals, anthropogenic influences and a correlation to bromine accumulation. Earth Planet Sci. Lett. 202, 435–451.
Sabatino, N., Ferraro, S., Coccioni, R., Bonsignore, M., Del Core, M., Tancredi, V., Sprovieri, M., 2018. Mercury anomalies in upper Aptian-lower Albian sediments from the Tethys realm. Palaeogeogr. Palaeoclimatol. Palaeoecol. 495, 163–170.
Sanei, H., Grassby, S.E., Beauchamp, B., 2012. Latest Permian mercury anomalies. Geol. 40, 63–66.
Santana, W., Pinheiro, A.P., Silva, C.M.R., Saraiva, A.A., 2013. A new fossil caridean shrimp (Crustacea: Decapoda) from the cretaceous (albian) of the Romualdo formation, Araripe basin, northeastern Brazil. Zootaxa 3620, 293–300.
Saraiva, A.A.F., Hessel, M.H., Guerra, N.C., Fara, E., 2007. Concreções calcárias na formação Santana, Bacia do Araripe: Uma proposta de classificação. Est. Geol. UFPE 17, 40–57.
Saraiva, A.A.F., Barros, O.A., Bantim, R.A.M., Lima, F.J., 2015. Guia para trabalhos de campo em paleontologia na Bacia do Araripe, 2ª Ed. URCA. Crato, p. 88.
Saraiva, A.A.F., Lima, F.J., Bantim, R.A.M., Vila Nova, B.C., Sayao, J.M., Kellner, A.W.A., 2016. Sítio Baixa Grande? Nova localidade fossilífera para a formação Romualdo (Grupo Santana), Bacia do Araripe. Cad. Cult. Ciênc. URCA 15, 3–18.
Sayão, J.M., Kellner, A.W.A., 2006. Novo esqueleto parcial de pterossauro (Pterodactyloidea, Tapejaridae) do Membro Crato (Aptiano), Formação Santana, Bacia do Araripe, nordeste do Brasil. Est. Geol. UFPE 16, 16–40.
Schobben, M., Ullmann, C.V., Leda, L., Korn, K., Struck,U., Reimold, W.U., Ghaderi , A., Algeo , T.J., Korte, C., 2026. Discerning primary versus diagenetic signals in carbonate carbon and oxygen isotope records: An example from the Permian-Triassic boundary of Iran. Chem. Geol. 422, 94-107.
Sial, A.N., Peralta, S., Ferreira, V.P., Toselli, A.J., Aceñolaza, F.G., Parada, M.A., Gaucher, C., Alonso, R.N., Pimentel, M.M., 2008. Upper cambrian carbonatesequences of the Argentine precordillera and the steptoean C-isotope positive excursion (SPICE). Gondwana Res. 13, 437–452. https://doi.org/10.1016/j.gr.2007.05.001.
Sial, A.N., Lacerda, L.D., Ferreira, V.P., Frei, R., Marquillas, R.A., Barbosa, J.A., Gaucher, C., Windmöller, C.C., Pereira, N.S., 2013. Mercury as a proxy for volcanic activity during extreme environmental turnover: the Cretaceous-Paleogene transition. Palaeogeogr. Palaeoclimatol. Palaeoecol. 387, 153–164.
Sial, A.N., Chen, J., Lacerda, L.D., Peralta, S., Gaucher, C., Frei, R., Cirilli, S., Ferreira, V. P., Marquillas, R.A., Barbosa, J.A., Pereira, N.S., Belmino, I.K.C., 2014. High-resolution Hg chemostratigraphy: a contribution to the distinction of chemical fingerprints of the Deccan volcanism and Cretaceous-Paleogene Boundary impact event. Palaeogeogr. Palaeoclimatol. Palaeoecol. 414, 98–115.
Sial, A.N., Chen, J., Lacerda, L.D., Frei, R., Tewari, V.C., Pandit, M.K., Gaucher, C., Ferreira, V.P., Cirilli, S., Peralta, S., Korte, C., Barbosa, J.A., Pereira, N.S., 2016. Mercury enrichment and Hg isotopes in Cretaceous–Paleogene boundary successions: links to volcanism and palaeoenvironmental impacts. Cretac. Res. 66, 1–22.
Sial, A.N., Chen, J., Lacerda, L.D., Frei, R., Higgins, J.A., Tewari, V.C., Gaucher, C., Ferreira, V.P., Cirilli, S., Korte, C., Barbosa, J.A., Pereira, N.S., Ramos, D.S., 2018. Chemostratigraphy across the cretaceous-paleogene (K-pg) boundary: testing the impact and volcanism hypotheses. In: Sial, A.N., Gaucher, C., Ramkumar, M., Ferreira, V.P., Org (Eds.), Chemostratigraphy across Major Chronological Boundaries. John Wiley and Sons Inc., New Jersey, pp. 223–257.
Silveira, A.C., Varejão, F.G., Neumann, V.H., Sial, A.N., Assine, M.L., Ferreira, V.P., Fambrini, G.L., 2014. Quimioestratigrafia de carbono e oxigênio dos carbonatos lacustres aptianos da serra do Tonã, subbacia de Tucano Norte, NE do Brasil. Est. Geol. UFPE 24 (2), 47–63, 2014.
Tomé, M.E.T.R., Filho, M.F.L., Neumann, V.H.M.L., 2014. Taxonomic studies of non-marine ostracods in the lower cretaceous (Aptian-Lower albian) of post-rift sequence from Jatobá and Araripe basins (northeast Brazil): stratigraphic implications. Cretac. Res. 48, 153–176.
Valença, L.M.M., Neumann, V.H., Mabessone, J.M., 2003. An overview on Callovian-Cenomanian intracratonic basins of Northeast Brazil: onshore stratrigraphic record of the opening of the southern Atlantic. Geol. Acta 1 (3), 261–275.
Varejão, F.G., Warren, L.V., Perinotto, J.A.J., Neumann, V.H., Freitas, B.T., Almeida, R. P., Assine, M.L., 2016. Upper Aptian mixed carbonate-siliciclastic sequences from Tucano Basin, Northeastern Brazil: implications for paleogeographic reconstructions following Gondwana break-up. Cretac. Res. 67, 44–58.
Weissert, H., 1989. C-isotope stratigraphy, a monitor of paleoenvironmental change: a case study from the early Cretaceous. Surv. Geophys. 10, 1–61.
Weissert, H., Erba, E., 2004. Volcanism, CO_2 and palaeoclimate: a Late Jurassic-Early Cretaceous carbon and oxygen isotope record. J. Geol. Soc. 161, 695–702.
Wilson, P.A., Norris, R.D., 2001. Warm tropical ocean surface and global anoxia during the mid-Cretaceous period. Nature 412, 425–429.
Yeomans, J.C., Bremner, J.M., 1998. A rapid and precise method for routine determination of carbon in soil. Commun. Soil Sci. Plant Anal. 19, 1467–1476.